scientific reports

Check for updates

OPEN

Canine mesenteric lymph nodes (MLNs) characterization by sc-RNAseq: insights compared to human and mouse MLNs

Beatriz Miguelena Chamorro[1,2], Sodiq Ayobami Hameed[2], Jean-Baptiste Claude[2], Lauriane Piney[2], Ludivine Chapat[2], Gokul Swaminathan[2], Hervé Poulet[2], Karelle De Luca[2], Egbert Mundt[2] & Stéphane Paul[1,3]✉

In the human and veterinary fields, oral vaccines generate considerable interest. In dogs, these vaccines are newly developed, and understanding their mechanisms is crucial. Mesenteric lymph nodes (MLNs) and Peyer's patches (PPs) are important sites for gastrointestinal mucosal induction, yet canine MLNs lack sufficient information. To address this, we collected MLN samples from healthy dogs, performed flow cytometry to characterize immune cells, and conducted single-cell RNA sequencing (scRNA-seq) to explore subpopulations, particularly B and T lymphocytes. This effort enabled the characterization of canine MLN's main cell populations and the construction of a predictive atlas, as well as the identification of particularities of this area.

Keywords Mucosal immune system, Canine, MLNs, Flow cytometry, Single cell-RNAseq

Oral vaccines have proven to be a convenient and effective method for combating mucosal pathogens in dogs, as demonstrated by the success of vaccines targeting oral rabies[1] and *B. bronchiseptica*[2]. These vaccines target the oral mucosa and the gut-associated lymphoid tissue (GALT) eliciting robust local mucosal immune responses. The Peyer's Patches (PPs) and mesenteric lymph nodes (MLNs) are key components of the inductive sites of the GALT, initiating and amplifying immune responses[3]. However, while a complete characterization of canine PPs has been recently published by our group[4], details on canine MLN remain partially unexplored. Previous studies on canine lymph nodes have largely focused on diagnostic techniques for tumor examination, such as colonoscopy[5] or tomography[6,7]. Moreover, flow cytometry has been employed to investigate specific cell markers, such as lymphocytes[8] as well as in combination with myeloid cell markers[9] or to detect canine $CD4^+CD8^+$ double-positive (dp) T cells[10]. Finally, canine MLNs shape and structure were briefly described almost forty years ago in a study focusing on sensory nerves. This study provided valuable insights into the architecture of canine lymph nodes, including the presence of germinal centers and medullary cords[11]. Nevertheless, there remains a need for a more profound comprehension of the canine lymph node populations in a healthy state. Recent technological advancements, notably in techniques like flow cytometry and single-cell RNA sequencing, have allowed us to study immune cell markers and visualize B and T cell subpopulations within the MLNs. Our research enhances our understanding of the mucosal immune system in dogs, while it also holds significant implications for various areas such as canine oral vaccines, enteropathies, and the use of dogs as models for human diseases.

Materials and methods

Animals

The MLNs used in this study were obtained from healthy dogs housed in the animal facilities of Boehringer Ingelheim Animal Health. These dogs, which had participated in prior research projects, provided the MLNs for our study after those unrelated studies were completed. In particular, the dogs involved were all healthy females beagles aged between 6 months and 1 year, and the previous procedures they underwent did not specifically involve or directly affect their intestinal health. Specifically, two dogs MLNs were used for flow cytometry, and the

[1]CIRI – Centre International de Recherche en Infectiologie, Team GIMAP (Saint-Etienne), Université Claude Bernard Lyon 1, Inserm, U1111, CNRS, UMR5308, ENS Lyon, UJM, 69007 Lyon, France. [2]Boehringer Ingelheim, Global Innovation, Saint-Priest, France. [3]CIC Inserm 1408 Vaccinology, 42023 Saint-Etienne, France. ✉email: stephane.paul@chu-st-etienne.fr

MLNs of four dogs were used for the scRNA-seq experiments. The experimental protocol was designed in accordance with French law (Decree Number 2001-464 29/05/01) and the recommendations of the European Economic Community (86/609/CEE) for the care and use of laboratory animals (Permit No. #23498-2020010715103375). The study has been reported in accordance with ARRIVE guidelines and is approved by the PLEXAN ethical committee (Agreement Number D180801).

Sample processing and flow cytometry

The MLN from two healthy dogs from the animal facilities of Boehringer Ingelheim were sampled and processed for flow cytometry. Briefly, the MLNs were sampled and minced, followed by dissociation with gentleMACS™ Dissociator (Miltenyi Biotec, 130-096-427). The resulting cell suspension was filtered, centrifuged, and resuspended in complete RPMI (Gibco™ 52400041). The cells were then layered onto a percoll density gradient (Cytiva, 17-0891-02), and the lymphocyte ring was collected. The cells were counted and plated in deep 96-well plates at a density of 500,000 cells/well. Flow cytometry staining was performed as previously described[4], using the surface and intracellular antibodies listed in Table Supp. 1. The samples were analyzed using the CYTEK Aurora, and the data obtained were analyzed with FlowJo version 10.8.1.

sc-RNAseq library preparation

For sc-RNAseq, MLNs from four healthy dogs from the animal facilities of Boehringer Ingelheim were sampled and processed as described above. The scRNA-seq library preparation was performed following the manufacturer's instructions using the Chromium Next GEM Single Cell 3' Reagents kits v3.1 (10 × Genomics, USA). Briefly, 20,000 cells were loaded into the Chromium Controller and the subsequent steps were carried out exactly as previously described[4]. The libraries were sequenced, resulting in FastQ files containing sequenced reads categorized as Read1, Index and Read2.

Bio-informatic analysis

The bioinformatic analysis of the scRNA-seq data was carried out using the CLC Genomics Workbench V21 software. The Cell Ranger pipeline was utilized for preprocessing and downstream analysis, with the dog (*Canis lupus familiaris*) genome (Ensembl ROS_Cfam_1.0; GCA_014441545.1) as the reference. The reads underwent demultiplexing and trimming, followed by mapping against the *Canis lupus familiaris* genome and quality control, as previously detailed[4]. Clustering was performed using principal component analysis (PCA) and visualized using the UMAP plot Leiden resolution of 0.3 and annotation was performed using databases such as CellMarker and PanglaoDB. Downstream analysis involved identifying cell subpopulations through marker gene expression, leading to the design of an immune cell atlas of the MLNs.

Results

Flow cytometry analysis was performed on samples gated based on the expression of $CD3^+$ for T cells and $CD21^+$ for B cells, exhibiting the mean frequency (%) of parents of the two animals (Fig. 1). The isolated lymphocytes comprised 49.95% T cells and 36.3% B cells. Among T cells, they were further categorized into $CD4^+$ T helper cells (74.4%) and $CD8^+$ cytotoxic T cells (13.3%), with a very small population of dp $CD4^+CD8^+$ T cells (1.16%). Bcl6 was used as a marker to identify follicular cells while FOXP3 to identify a regulatory phenotype of T helper cells. However, the expression of Bcl6 in both T and B cells was barely detectable (Fig. 1). Meanwhile, the expression of $FOXP3^+$ was present in 11.1% of the total T helper cells.

Next, in-depth analysis was performed using sc-RNASeq at the gene level. Clustering analysis identified nine distinct clusters based on gene expression differences (Fig. 2A). Known canonical cell type-specific markers were manually annotated to identifypro specific cell types within each cluster (Fig. 2B). The mesenteric lymph node contained seven identified cell types, including T cells, B cells, plasma cells, natural killer (NK) cells, ILCs, epithelial cells, and fibroblasts (Fig. 2B). These cells were annotated using the same expression markers that were previously employed for the annotation of canine Peyer's patches[4]. B cells were annotated based on the expression of CD19, MS4A1 (encoding CD20), CD79A and CD79B. T cells were annotated based on the expression of CD3D/CD3E and LCK (lymphocyte-specific protein tyrosine kinase). In addition, plasma cells were annotated based on the expression of B cell markers and SDC-1 (CD138)[12,13]. Furthermore, NK cells were annotated based on the expression of NKG7, GZM, PRF1, CD2 and CD160[12,13]. Epithelial cells were characterized by epithelial cell adhesion molecule (EpCAM) expression, and fibroblasts were annotated based on PDGFRA expression[14]. ILCs were annotated as $CD45^+$ cells (expressing protein tyrosine phosphatase, receptor type, C "PTPRC") that lack the expression of distinct T-cell and B-cell and other immune cell lineage-specific markers but with specific expression of IL7R (CD127)[15]. Overall, ~ 99% of the cells were successfully annotated, however no myeloid cells were captured in the dataset.

T cells represented 48.7% of the total detected cells and $CD4^+$ T cells accounted for the majority, representing approximately 88% of total T cells. $CD8^+$ T cells comprised 7%, and the remaining $CD3^+$ cells did not exhibit clear CD4 or CD8 expression. Further exploration to delineate subpopulations revealed that a large proportion expressed both CCR7 and CD62L, indicative of central memory T cells (Fig. 3A). These $CCR7^+$ $CD62L^+$ $CD4^+$ T cells represented the largest population of T cells (55%) and could be categorized as central memory T cells[16]. Another subpopulation of CD4 T cells expressing ICOS, PD-1 and/or CXCR5 was annotated as T-follicular helper cells (TFH cells), as these were lineage-specific markers known to delineate the TFH cells[12,17]. Based on the relative expression of the above markers, we had 2 subpopulations of TFH cells: $ICOS^+$ $PD\text{-}1^+$ $CXCR5^+$ TFH cells (18%) and $ICOS^+$ $PD\text{-}1^{lo/-}$ $CXCR5^{lo/-}$ TFH cells (14%). A small subpopulation of CD4 T cells (1.5%) expressed TOP2A, PCLAF and MCM5 which were markers of cell proliferation or cell cycle (17) and were annotated as proliferating CD4 T cells. Other CD4 T cells represented only 0.1% of the total T-cell population; the phenotype

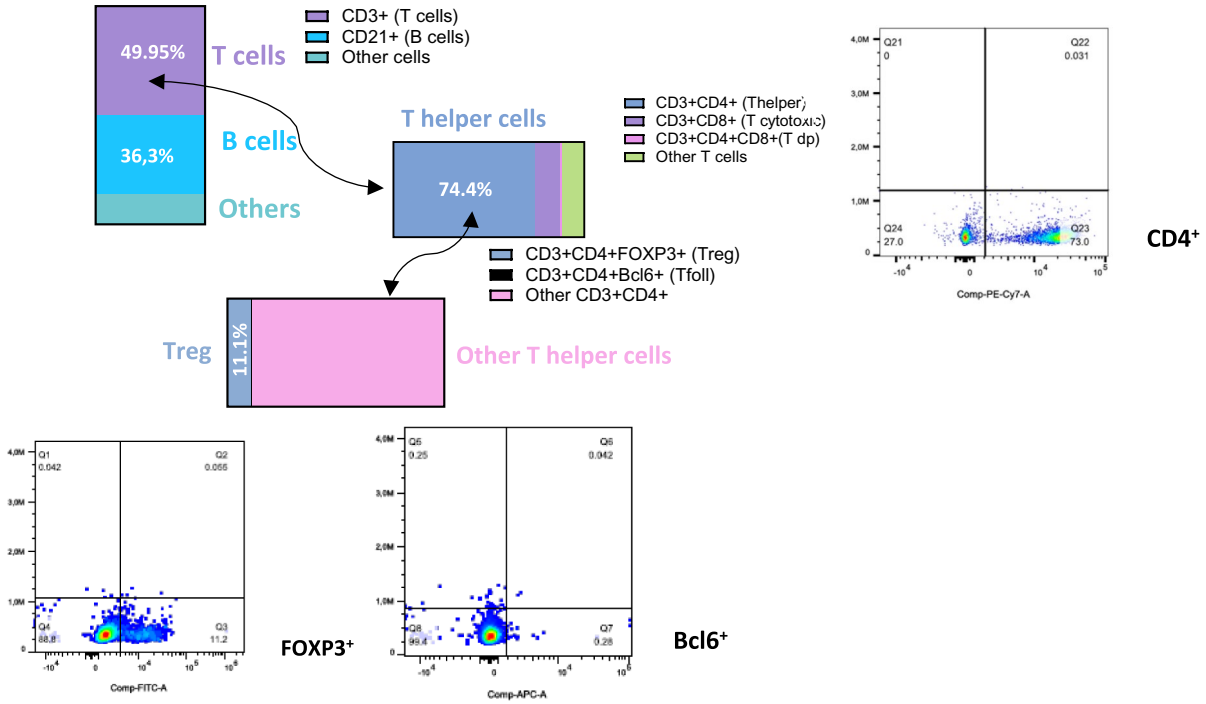

Fig. 1. T and B cell populations of the canine MLNs by flow cytometry. Proportions of T and B cells: T cells accounted for 49.95% and B cells for 36.3% of the cell population analyzed. T cells were further separated into $CD8^+$ and $CD4^+$, and 11.1% of $CD4^+$ T cells had a regulatory phenotype-FOXP3. Moreover, none of the analyzed cells expressed Bcl6.

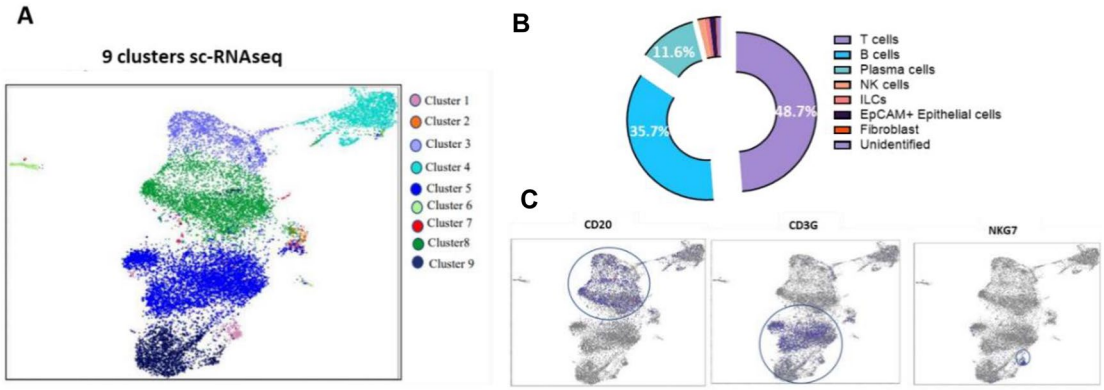

Fig. 2. Clusters and cell-type classification by sc-RNAseq. (**A**) Cluster classification: 9 clusters were identified with a Leiden resolution of 3.0, making it possible to classify different cell populations. (**B**) Cell populations identified: 7 cell populations were identified on the basis of gene expression profile. T cells, B cells, and plasma cells predominated. (**C**) Marker expression: the expression of markers such as CD20, CD3G and NKG7 were visualized across the identified clusters, facilitating cell type identification.

of these cells could not be specifically delineated (Fig. 3A). B cells were annotated based on the expression CD19, CD20, CD79A and/or CD79B, and were detected for approximately 36% of the total cell population and four subtypes were identified (Fig. 3B). Firstly, a subpopulation of B cells was found to be $FCER2^+$ (encoding CD23) $CXCR5^+$ and these cells were putatively annotated as follicular B cells[16]. A second population of B cells expressed AICDA which defines cells potentially undergoing affinity maturation[17]. Some of these cells expressed proliferation markers (TOP2A and PCLAF) together with the AICDA, indicative of proliferative germinal center (GC) cells, and these were defined as dark zone (DZ) germinal center B cells[18]. The other $AICDA^+$ cells did not express proliferation markers and were categorized as GC light zone (LZ) B cells since they expressed AICDA and CXCR5, indicative of GC cells potentially interacting with TFH cells in the light zone[18]. A third population of B cells represented proliferating B cells which expressed proliferation markers (without AICDA and CXCR5). Overall, in the mesenteric lymph nodes, the subtype distribution of a total of 5.770 B cells was 57% follicular B cells, 16% dark zone GC B cells, 14% light zone GC B cells, and 8.5% proliferating B cells (Fig. 3B). Finally, an

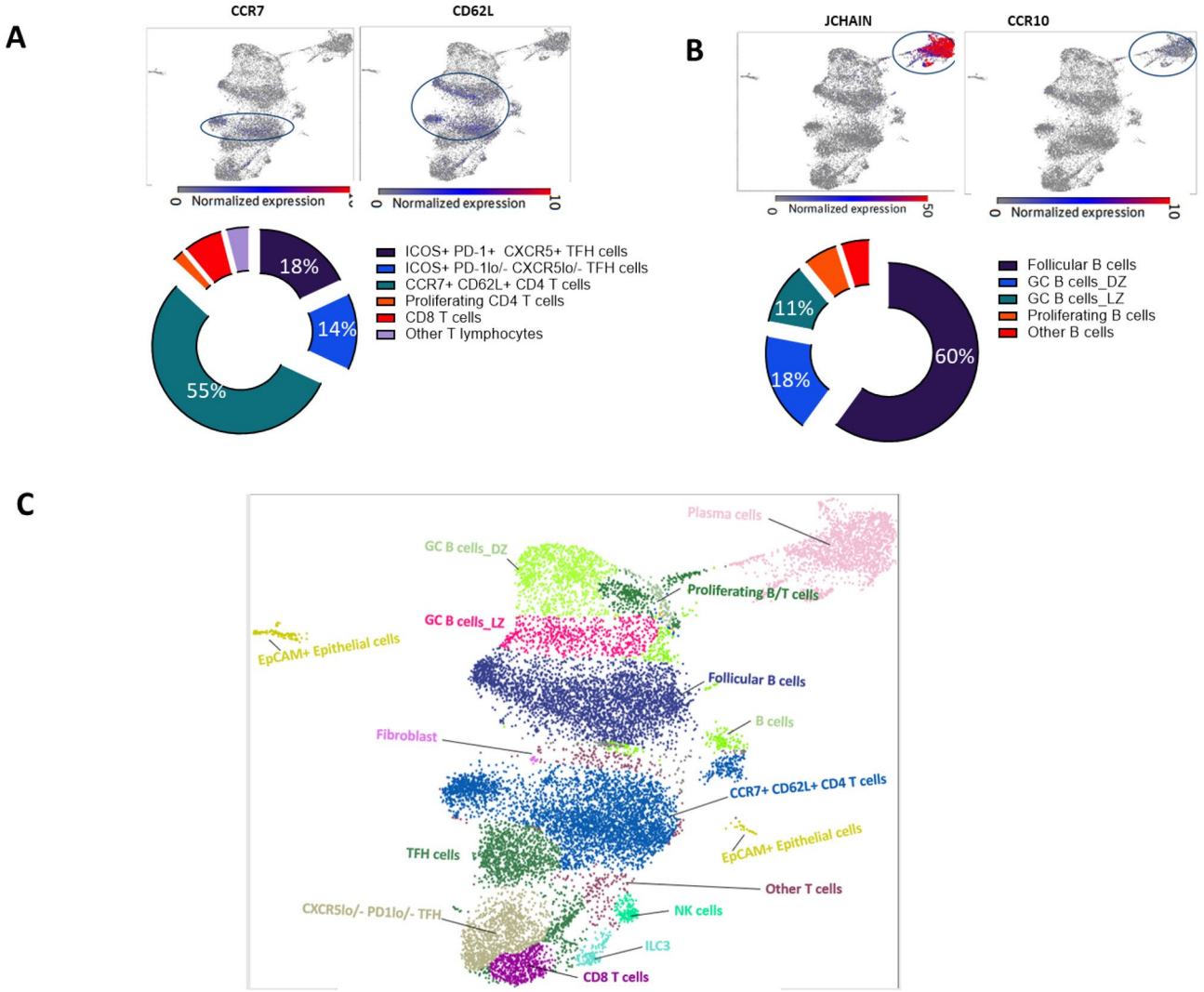

Fig. 3. B- and T-cell subpopulations, and the canine MLs atlas. (**A**) T-cell subpopulations: the distribution of different T-cell subpopulations is presented as a pie chart, with the corresponding percentages and example of marker expression of CCR7 and CD62L are shown (**B**) B-cell subpopulations: the distribution of different B-cell subpopulations is shown as a pie chart, with the corresponding percentages and example of marker expression of JCHAIN and CCR10 are shown (**C**) MLN Atlas: We propose an annotation of the immune cells identified within clusters, based on the specific expression patterns of marker genes. Abbreviations: CCR7, C–C chemokine receptor type; CD62L, cluster of differentiation 62 L-selectin; CXCR5, C-X-C chemokine receptor 5; DZ, dark zone; EpCAM, epithelial cell adhesion molecule; GC, germinal center; ILC3, innate lymphoid cells group 3; LZ, light zone; NK, natural killer cells; PD-1, programmed cell death protein 1; TFH, T follicular helper cell. CD62L, cluster of differentiation 62 L-selectin; CCR7, C–C chemokine receptor type; CXCR5(lo), C-X-C chemokine receptor 5 (low); ICOS, inducible T-cell costimulator; PD-1(lo), programmed cell death protein 1 (low); TFH, T follicular helper cells.

immune cell atlas based on the identified populations and subpopulations was developed to provide an overview of the immune cell types and subtypes present in the mesenteric lymph nodes of healthy dog (Fig. 3C).

Discussion

We have successfully characterized for the first time the main population of the mesenteric lymph nodes in the dog, which play a crucial role in the induction and amplification of immune responses within the GALT[3]. Our observations revealed that canine mesenteric lymph nodes are predominantly populated by CD4 T cells, with a reasonable proportion of CD8 T cells. A recent study has reported the CD4 T cells from the mesenteric lymph node to be predominantly of the $ICOS^{hi}$ $CXCR5^{+}$ TFH and $CCR7^{+}$ $CD62L^{+}$ central memory phenotypes in human[16]. Interestingly, this is in concordance with our results as we have observed these two CD4 T-cell phenotypes to represent more than 70% of the CD4 T cells. In contrast, in canine Peyer's patches, the proportion of these two cell populations is lower, accounting for less than 30%[4].

Similar to our findings in the study of canine Peyer's patches[4], the analysis of protein levels using flow cytometry and gene expression levels using sc-RNAseq allowed us to obtain comparable results regarding the proportions of B and T cells, as well as the subpopulations of T helper and cytotoxic T cells. However, the specific population of dp $CD4^+$ $CD8^+$ T cells was barely undetectable by flow cytometry (1.16%) and not detected by gene expression in sc-RNAseq. This aligns with previous observations by Rabiger et al., where the percentage of dp T cells in mesenteric lymph nodes was lower than 1% compared to Peyer's patches (3%). The small population size may explain why it was not detected by sc-RNAseq. Similarly, innate cells were not detected in canine mesenteric lymph nodes, as seen in the study of canine Peyer's patches and other studies, indicating that previous enrichment techniques would be necessary[4,19]. Interestingly, NK cells were detected in canine MLNs, while the same markers (CD2, CD160, GZM, and PRF-1) were also detected in canine Peyer's patches. However, the simultaneous expression of CD8 in this population prevented its classification as NK cells, unlike in mesenteric lymph nodes[4].

We identified key zones in mesenteric lymph nodes, such as germinal centers with distinct dark and light zones, based on the expression of specific genes by cell populations. However, further verification of the structure and distribution of these zones is required using immunofluorescence. Follicular cells, crucial in germinal centers, were identified using markers such as ICOS, PD-1, and/or CXCR5. CXCR5, in particular, facilitates B cell trafficking to the follicle in response to CXCL13 (18).

Flow cytometry analysis revealed the absence of Bcl6 expression, which was further confirmed by sc-RNAseq. Bcl6 is a transcription factor that commits CD4 T cells to the Tfh phenotype[20] and plays a critical role in B cell differentiation and germinal center development[21]. Particularly, Bcl6 plays an essential role on the interaction of B and T cells inside the follicle leading to GC formation[22]. Notably, a recent article demonstrated that in COVID-19, the loss of germinal centers coincides with the depletion of Bcl-6^+ B cells and impaired $Bcl6^+$ Tfh cells[23]. However, the implications of the absence of Bcl6 expression in canine lymph nodes remain unknown, especially considering its presence in canine Peyer's patches and the expected migration between these areas.

Overall, this study provides an overview of the main cell populations in the canine MLNs, highlighting the prominence of T and B cells and the lack of innate cell discovery. It also raises new research questions: What are the implications of the absence of Bcl6 expression? Which other transcription factors are involved in the development of T follicular cells in canine lymph nodes?

Data availability

The datasets used and/or analysed during the current study available from the corresponding author on reasonable request.

Received: 6 May 2024; Accepted: 27 August 2024
Published online: 31 August 2024

References

1. Wallace, R. M. *et al.* Early release—Role of oral rabies vaccines in the elimination of dog-mediated human rabies deaths—Volume 26, number 12—December 2020—Emerging infectious diseases journal—CDC. *Emerg. Infect. Dis.* **26**, e201266 (2020).
2. Scott-Garrard, M., Wang, X., Chiang, Y. & David, F. Thirteen-month duration of immunity of an oral canine vaccine against challenge with Bordetella bronchiseptica. *Vet. Rec. Open* **7**, e000423 (2020).
3. McGhee, J. R. & Fujihashi, K. Inside the mucosal immune system. *PLoS Biol.* **10**, e1001397 (2012).
4. Miguelena Chamorro, B. *et al.* Characterization of Canine Peyer's patches by multidimensional analysis: Insights from immunofluorescence, flow cytometry, and single-cell RNA sequencing. *ImmunoHorizons* **7**, 788–805 (2023).
5. Sudan, D., Miller, S. & Mellinger, J. Colonoscopic indirect lymphangiography in a canine model. *Surg. Endosc.* **7**, 96–99 (1993).
6. Beukers, M., Grosso, F. V. & Voorhout, G. Computed tomographic characteristics of presumed normal canine abdominal lymph nodes. *Vet. Radiol. Ultrasound* **54**, 610–617 (2013).
7. Teodori, S. *et al.* Computed tomography evaluation of normal canine abdominal lymph nodes: Retrospective study of size and morphology according to body weight and age in 45 dogs. *Vet. Sci.* **8**, 44 (2021).
8. Riondato, F. *et al.* Flow cytometric features of B- and T-lmphocytes in reactive lymph nodes compared to their neoplastic counterparts in dogs. *Vet. Sci.* **10**, 374 (2023).
9. Parys, M., Bavcar, S., Mellanby, R. J., Argyle, D. & Kitamura, T. Use of multi-color flow cytometry for canine immune cell characterization in cancer. *PLOS One* **18**, e0279057 (2023).
10. Rabiger, F. V. *et al.* Canine tissue-associated CD4+CD8α+ double-positive T cells are an activated T cell subpopulation with heterogeneous functional potential. *PLoS One* **14**, e0213597 (2019).
11. Popper, P., Mantyh, C. R., Vigna, S. R., Maggio, J. E. & Mantyh, P. W. The localization of sensory nerve fibers and receptor binding sites for sensory neuropeptides in canine mesenteric lymph nodes. *Peptides* **9**, 257–267 (1988).
12. Franzén, O., Gan, L.-M. & Björkegren, J. L. M. PanglaoDB: A web server for exploration of mouse and human single-cell RNA sequencing data. *Database* **2019**, baz046 (2019).
13. Zhang, X. *et al.* Cell Marker: A manually curated resource of cell markers in human and mouse. *Nucleic Acids Res.* **47**, gky900 (2018).
14. Fawkner-Corbett, D. *et al.* Spatiotemporal analysis of human intestinal development at single-cell resolution. *Cell* **184**, 810-826. e23 (2021).
15. Björklund, Å. K. *et al.* The heterogeneity of human CD127+ innate lymphoid cells revealed by single-cell RNA sequencing. *Nat. Immunol.* **17**, 451–460 (2016).
16. James, K. R. *et al.* Distinct microbial and immune niches of the human colon. *Nat. Immunol.* **21**, 343–353 (2020).
17. Madissoon, E. *et al.* scRNA-seq assessment of the human lung, spleen, and esophagus tissue stability after cold preservation. *Genome Biol.* **21**, 1 (2019).
18. Crotty, S. T follicular helper cell biology: A decade of discovery and diseases. *Immunity* **50**, 1132–1148 (2019).
19. Sparling, B. A. *et al.* Unique cell subpopulations and disease progression markers in canines with atopic dermatitis. *J. Immunol. Baltim. Md* **1950**(209), 1379–1388 (2022).
20. Crotty, S., Johnston, R. J. & Schoenberger, S. P. Effectors and memories: Bcl-6 and Blimp-1 in T and B lymphocyte differentiation. *Nat. Immunol.* **11**, 114–120 (2010).
21. Crotty, S. Revealing T follicular helper cells with BCL6. *Nat. Rev. Immunol.* **21**, 616–617 (2021).

22. Liu, D. *et al.* BCL6 controls contact-dependent help delivery during follicular T-B cell interactions. *Immunity* **54**, 2245-2255.e4 (2021).
23. Kaneko, N. *et al.* The loss of Bcl-6 expressing T follicular helper cells and the absence of germinal centers in COVID-19. *SSRN Electron. J.* https://doi.org/10.2139/ssrn.3652322 (2020).

Author contributions

B.M.C., S.A.H., J.B.C., L.P., L.C. have performed the experiments. B.M.C., G.S., H.P., K.D.L., E.G., S.P. have written the manuscript.

Competing interests

The authors declare no competing interests.

Additional information

Supplementary Information The online version contains supplementary material available at https://doi.org/10.1038/s41598-024-71310-9.

Correspondence and requests for materials should be addressed to S.P.

Reprints and permissions information is available at www.nature.com/reprints.

Publisher's note Springer Nature remains neutral with regard to jurisdictional claims in published maps and institutional affiliations.